ELSEVIER

Journal of Molecular Catalysis A: Chemical 194 (2003) 115–135

JOURNAL OF MOLECULAR CATALYSIS A: CHEMICAL

www.elsevier.com/locate/molcata

Propane and propylene adsorption effects over MoO_x-based catalysts induced by low levels of alkali doping

Rick B. Watson, Umit S. Ozkan*

Department of Chemical Engineering, The Ohio State University, Columbus, OH 43210, USA

Received 17 June 2002; accepted 12 August 2002

Abstract

The induced effects of low-level alkali promotion are studied in order to obtain a better understanding of the way the MoO_x activity, altered by the presence of potassium, relates to the adsorption and reactivity of propane and propylene under various conditions. Non-steady-state and steady-state isotopic transient kinetic analyses (SSITKAs) show changes in lattice-oxygen mobility caused by the presence of potassium. Differential scanning calorimetry was used to determine the heat effects associated with propylene adsorption. The heat associated with the reversible and irreversible adsorption of propylene decreases with the addition of potassium. This information further corroborates the relationship between potassium addition and the decreased reactivity for propylene as elucidated in reaction experiments. Electron spin resonance was used to investigate changes in Mo(V) species upon contact with propane under different conditions as a probe for the electronic properties of the supported MoO_x species. ESR experiments indicate that it may be possible that potassium stabilizes the MoO_x domains in a more "reduced" state, Mo(V). Together with in situ-DRIFTS experiments, it is found that potassium cannot only affect the transformation of propylene over MoO_x catalysts, but also change the interaction of the catalyst with propane, altering propane activation steps.

Keywords: DRIFTS; ESR; Propane; Propylene; Molybdenum; Silica–titania

1. Introduction

A major challenge in heterogeneous catalysis is the design and development of new catalysts for selective transformation of lower hydrocarbons [1]. The oxidative dehydrogenation (ODH) of lower alkanes to form alkenes has been extensively studied [2–5] for such purpose. In particular, the ODH of propane is attractive as a process to produce propylene, given its high demand for the production of polypropylene, acrylonitrile, and propylene oxide. However, ODH selectivity is limited considering the high reactivity of propylene toward further oxidation. As discussed by Kung in a review article [2], the limitation arises from consecutive reactions, namely propane → propylene and propylene → CO_x. It was shown that, perhaps on all catalysts, the rate for the second reaction could be 5–10 times higher than that of the first reaction. In fact, more recent work by Khodakov et al. [6,7] has determined the relative rate of propylene combustion to be 20 times as high as the rate of propylene formation over vanadium based catalysts. Chen et al. has also measured the same rate to be 10–20 times higher on molybdenum-based catalysts [8,9]. Furthermore, the authors have commented on the likelihood of similar active sites being responsible for both reactions.

* Corresponding author. Tel.: +1-614-292-6623; fax: +1-614-292-3769.
E-mail address: ozkan.1@osu.edu (U.S. Ozkan).

1381-1169/02/$ – see front matter © 2002 Elsevier Science B.V. All rights reserved.
PII: S1381-1169(02)00476-4

This limitation in propane ODH has led to, at best, a general description of the qualities that a selective catalyst must possess. Selectivity requires careful control of the abundance of active oxygen and of the adsorption/desorption characteristics to avoid re-adsorption of the formed propylene. There is a combined influence of the redox and acid–base properties of the surface of the oxides used for propane ODH. Intermediate reducibility, weak Lewis acid centers, and oxygen mobility represent the essential requirements for selective ODH; as they are consistent with the trends in ODH rates observed on VO_x, MoO_x, and WO_x-based catalysts [10]. However, quantitative correlations between these properties and catalytic performance cannot easily be obtained and these characteristics are therefore usually expressed in literature as a "good-mix" or "favorable balance" between acid–base characteristics and redox behavior [11–13]. The "favorable" oxygen that can provide this requirement is that which binds strongly enough to the surface to have attenuated oxidizing strength but weakly enough to oxidize the reactant molecule selectively. Over supported transition-metal oxides, the species of interest exist in the form of M=O, M–O–M, or M–O-support bonds, where M is the supported transition-metal. The nature of the active oxygen will certainly depend upon transition-metal loading, dispersion, support effects, and the addition of modifiers, such as potassium.

The accompanying increase in activity and/or selectivity in partial oxidation reactions with the use of alkali (Li, Na, K, Rb, and Cs) doping has been widely studied and offers a way to adjust the redox and acidic properties of supported transition-metal oxides [14–22]. The positive effects of alkali promotion arise from the ability of the alkali to alter oxidation/reduction behavior, affect surface acidity, and/or cause a synergy between alkali and transition-metal oxide phases. Recent work from our laboratory has examined the structural changes associated with alkali promotion at low levels [23]. The presence of potassium significantly alters the electronic structure of the surface MoO_x domains supported over the binary oxide of silica/titania. Data suggested that surface supported species, present as distorted octahedral MoO_x, become further distorted at low levels of alkali (K/Mo = 0.07). The MoO_x species at this level of alkali promotion, experiencing a decrease in Lewis acidity, could tend to be more reactive toward electronegative Si–O^- support ligands on the Si:Ti 1:1 support. The interaction of MoO_x domains with the binary oxide support, and consequently reactivity, can be altered with the addition of potassium. It was shown that small levels of alkali suppress the reducibility and Lewis acidity of the molybdenum species and possibly stabilize a lower oxidation state of Mo during the propane ODH reaction [24].

It this study, we continue to examine the induced effects of low-level alkali promotion in order to obtain a better understanding of the way the MoO_x reactivity, altered by the presence of potassium, relates to the adsorption and reactivity of propane and propylene under various conditions. Furthermore, the use of non-steady-state and steady-state isotopic transient kinetic analysis (SSITKA) was used to extend our discussion to changes in oxygen mobility caused by the presence of potassium. Differential scanning calorimetry was used to determine the heat effects associated with propylene adsorption. Diffuse reflectance infrared Fourier transform spectroscopy was used to characterize adsorbed species present in non-selective transformations of propane/propylene in an oxygen atmosphere. Electron spin resonance was used to investigate changes in Mo(V) species upon contact with propane under different conditions as a probe for the electronic properties of the supported MoO_x species. A summary of the observed effects is provided with relation to catalyst structure.

2. Experimental

2.1. Catalyst preparation

Catalysts were prepared using a "one-pot" modified sol–gel/co-precipitation technique. Ammonium heptamolybdate (AHM) (Mallinkrodt) was used for the molybdenum precursor. For silica–titania mixed and single oxides, tetraethylorthosilicate (TEOS) (Aldrich) and titanium(IV)isopropoxide (TIPO) (Aldrich) were used. This method is referred to as a "one-pot" sol–gel/co-precipitation and was described previously [24]. In this modified sol–gel method, calculated amounts of the silica and titania alkoxide precursors were placed in a ethanol/iso-propanol solvent with a 1:1 volume ratio and hydrolyzed with the appropriate amount of an aqueous solution containing the Mo

Table 1
Sol–gel catalysts

No.	Composition	Preparation	Surface area (m^2/g)
1	10% Mo/Si:Ti 1:1	Co-precipitation, sol–gel	229
2	10% (K/Mo = 0.035)/Si:Ti 1:1	Co-precipitation, sol–gel	164
3	10% (K/Mo = 0.07)Si:Ti 1:1	Co-precipitation, sol–gel	136
4	10% (K/Mo = 0.14)/Si:Ti 1:1	Co-precipitation, sol–gel	121
5	10% (K/Mo = 0.3)/Si:Ti 1:1	Co-precipitation, sol–gel	129
6	Si:Ti 1:1	Sol–gel hydrolysis	320

precursor. The aqueous solution added contained the stoichiometric amount of water necessary to hydrolyze all of the alkoxide precursors. For catalysts containing alkali, KOH was added to the aqueous solution to give the desired alkali/Mo molar ratio. Catalysts compared in this study contain 10 wt.% molybdenum supported on the mixed oxide of silica/titania with a molar ratio of 1 (Si:Ti 1:1). For the catalysts containing alkali, attention was focused on low-level promotion (K/Mo = 0.07 and 0.3). However, some studies were performed on a range of alkali-promoted catalysts to provide a better comparison. The catalysts are presented in Table 1. Catalysts numbered 1–5 are a series of molybdate catalysts with increasing K/Mo molar ratio at constant (10 wt.%) loading of Mo and a Si:Ti molar ratio of 1. Table entry number 6 is the Si:Ti 1:1 support prepared the same way with no molybdenum component. BET surface area measurement and nitrogen adsorption–desorption isotherms were recorded using a Micrometrics AccuSorb 2100E instrument.

2.1.1. Non-steady-state and steady-state isotopic transient kinetic analysis (SSITKA)

Oxygen isotopic exchange flow experiments were performed using a laboratory-made gas flow system described in detail elsewhere [25]. Catalyst samples (100 mg) were placed in a 1/4 in. i.d. U-tube quartz reactor and pre-treated under oxygen ($^{16}O_2$) flow at 550 °C for 1 h. A mixture of 10% $^{16}O_2$ in helium with a small amount of argon present (∼1%) was then passed over the samples and allowed to equilibrate. After steady mass spectrometer signals were obtained, the flow was switched to that containing 10% $^{18}O_2$ (Isotec) in helium and the exchange was carried out for 10 min at 500 °C. Oxygen species ($^{16}O_2$, ^{16}O, ^{18}O and $^{18}O_2$) and argon were monitored by a mass spectrometer (HP5890GC–MS) under helium carrier gas. The normalized concentration of each isotope for a given species was calculated by dividing the signal for that isotope by the sum of the signals for all the isotopes of that species.

For transient isotopic oxygen exchange, catalyst samples (100 mg) were pre-treated in 10% $^{16}O_2$ for 1 h at 500 °C followed by 1 h of evacuation at 10^{-7} Torr in a quartz U-tube reactor. The samples were then flushed under flowing helium for 1 h at 500 °C. A flow of 10% $^{18}O_2$ (Isotec) in helium with a small amount of argon (∼1%) was introduced and the exchange was carried out for 10 min at 500 °C.

Isotopic oxygen exchange in the presence of reaction was performed by establishing two gas-feed streams. The first contained 5% propane, 2.5% $^{16}O_2$, 91.5% He, and 1% argon. The second mixture contained 5% propane, 2.5% $^{18}O_2$, and 92.5% He. Experiments were performed in the same apparatus using 100 mg of sample starting with a pre-treatment under oxygen ($^{16}O_2$) flow at 550 °C for 1 h. The first reaction mixture was introduced and reaction was carried out in the U-tube reactor until steady-state was established at 500 °C at a flow rate of 25 cm^3/min. The flow was subsequently switched to that containing the oxygen isotope and the exchange was carried out for 10 min at 500 °C. During the exchange, no change in MS signals associated with propane or propylene was detected indicating that the switch did not perturb the steady-state of the reaction.

In the two sets of oxygen isotopic exchange experiments conducted at steady-state, it was necessary to determine if there was a significant contribution from a homogeneous scrambling to form ^{16}O ^{18}O in the gas phase. These “blank” experiments were performed in a U-tube reactor under the same conditions using a quartz wool plug roughly the same size as the catalyst bed. In these experiments, there was no detectable

formation of cross-labeled oxygen. Furthermore, during the blank experiment for isotopic oxygen exchange in the presence of reaction, there was no detectable formation of cross-labeled oxygen as well as no propane conversion associated with gas-phase reaction.

2.1.2. Differential scanning calorimetry (DSC)

Differential scanning calorimetry was performed using a Perkin-Elmer DSC-7 differential power unit. The unit consisted of aluminum sample and reference pans. Samples (50 mg) were placed in the sample aluminum pan and pretreated in 10% O_2 in nitrogen at 500 °C for 30 min followed by cooling to 100 °C under nitrogen. The experimental procedure involved switching between dry nitrogen and 5% propylene/nitrogen flow using a 4-port valve to measure the heat associated with both irreversible and reversible propylene adsorption. DSC thermograms were obtained at 100 °C. To account for the heat capacity difference between the flow of nitrogen and propylene/nitrogen, a series of switches were carried out under the same experimental conditions using an empty sample pan. The amount of measured heat corresponding to this heat capacity difference was then subtracted from that obtained during the experiments. The instrument was calibrated individually for each sample studied by the heat of fusion of indium metal (5 mg) as measured by placing the metal on top of the catalyst sample placed in the sample pan. This method corrects for differences in heat conduction between the catalyst samples and heat loss to the gas phase.

2.1.3. Diffuse reflectance infrared Fourier transform spectroscopy (DRIFTS)

DRIFTS of the studied catalysts were performed using a Bruker IFS66 instrument equipped with a DTGS detector and a KBr beamsplitter. Catalysts were placed in a sample cup inside a Spectratech diffuse reflectance cell equipped with KBr windows and a thermocouple mount that allowed direct measurement of the surface temperature. Spectra for each catalyst were averaged over 1000 scans in the mid-IR range (400–4000 cm^{-1}) to a nominal 2 cm^{-1} resolution. Prior to collecting spectrum, catalysts were pretreated under 10% oxygen in helium for 30 min at 400 °C surface temperature to remove adsorbed water and carbon dioxide. For propane and propylene adsorption experiments, background spectra were taken under a 1% O_2 in helium flow at various temperatures (150, 200, 250, 300, and 350 °C). Following background measurement, the samples were purged for 1 h under helium after which propane or propylene adsorption was performed for 1 h at 150 °C. The samples were then flushed for 1 h under helium flow at 150 °C. A 1% O_2 in helium flow was introduced and spectra were taken at each successive temperature after an equilibration time of 15 min.

2.1.4. Electron spin resonance (ESR)

Electron spin resonance (ESR) spectra were acquired on a Bruker ESP300 electron spin resonance spectrometer. For ESR spectrum taken under dehydrated conditions, a portion of prepared samples were re-calcined at 550 °C for 30 min under pure O_2 and maintained in the dehydrated state at 110 °C for 2 days prior to analysis. The spectra were obtained at room temperature with a Klystron frequency of 9.7 GHz and 100 kHz magnetic field modulation. A portion of prepared samples was also placed inside a quartz ESR tube (Wilmad) capable of sealing the sample under a gas atmosphere or vacuum. Dehydrated samples were subsequently purged at 10^{-3} Torr for 12 h after which 100 Torr of propane was introduced. ESR spectra were recorded after 15 min at room temperature under the propane atmosphere. Another set of propane "reduction" experiments were performed in which the samples were contacted with 500 Torr of propane at 400 °C for 30 min followed by evacuation at 10^{-3} Torr. ESR spectra were recorded under vacuum.

2.2. Oxidative dehydrogenation of propane and oxidation of propylene

The catalysts were tested in a fixed-bed, quartz reactor operating at ambient pressure. Reaction products were separated and analyzed online using a HP 5890 series II gas chromatograph containing FID and TCD detectors. Separations were performed using columns: (1) Hayesep D (8 ft × 1/8 in.) for hydrocarbons and partially oxygenated hydrocarbons; (2) Porapak Q (6 ft × 1/8 in.) and (3) molecular sieve 5 Å (6 ft × 1/8 in.) for N_2, O_2, CO, CO_2, and H_2O. Reactions were carried out at steady-state using 65 m^2 of catalyst surface area in the reactor. Catalyst samples were held in place by a quartz frit. The feed consisted of propane/oxygen/nitrogen or propylene/oxygen/nitrogen at a flow of 25 cm^3/min. The

concentration of the feed stream was maintained outside the flammability limits of propane/propylene–oxygen–nitrogen mixtures for all runs. The main products of the dehydrogenation reaction were propylene, methane, carbon dioxide, carbon monoxide, and water. The main products of propylene oxidation were acrolein, carbon dioxide, carbon monoxide, water and trace amounts of acrylic acid. To assure that the homogenous reactions were minimized, the dead volume of the quartz reactor was packed with quartz wool and ceramic beads to minimize any gas-phase effects that may occur in the presence of a catalyst.

3. Results and discussion

3.1. Propane ODH and propylene oxidation experiments

The (K/Mo)/Si:Ti 1:1 catalysts were compared in the propane ODH reaction using equal surface area loading (65 m^2) in the reactor and at a temperature of 550 °C. The feed percentages for these experiments were $N_2/C_3/O_2$: 92.5/5/2.5. Reaction data were taken after steady-state was reached. The variation of propylene formation rates with K/Mo ratio for these equal surface area tests are presented in Fig. 1. These are observed rates for propylene formation in that they are the summation of both formation from propane and its successive depletion that are observed during the reaction. The rates are seen to increase through a maximum between K/Mo = 0.07 and 0.14 and fall as K/Mo is increased to 0.3. Propylene oxidation experiments run under the same conditions ($N_2/C_3/O_2$: 92.5/5/2.5; 550 °C) revealed a propylene conversion rate that steadily decreased with K/Mo molar ratio. When propane and propylene oxidation experiments are compared under these identical conditions, a maximum exists in the ratio of propane to propylene conversion rates. This suggests that the increase in propylene formation at the low K/Mo molar ratios (0.07 and 0.14) during ODH experiments is due to a decreased reactivity toward propylene caused by the addition of alkali. In previous work, we have related

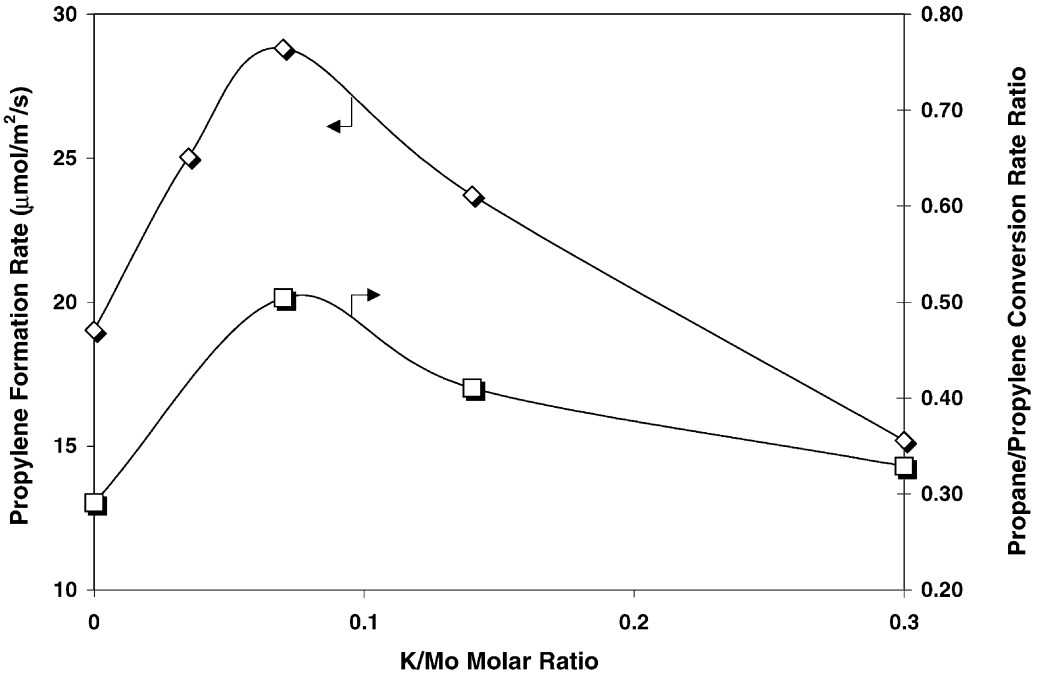

Fig. 1. Propylene formation rates (◇) of Mo/Si:Ti 1:1 catalysts with different K/Mo molar ratios. Reaction conditions: equal surface area reactions (65 m^2), $\%N_2/\%C_3/\%O_2$ 92.5/5/2.5, 25 cc/min. Propane/propylene conversion ratio (□) obtained under identical conditions. Reaction conditions: equal surface area reactions (65 m^2); $\%N_2/\%C_3{}^{2-}/\%O_2$: 92.5/5/2.5; 25 cc/min.

this behavior to the secondary effect induced by alkali promotion [24]. The surface oxygen species are affected by the presence of potassium and this, in turn, affects the rates of both propane activation and propylene combustion. The reactivity trends are related to a combination of the decrease in Lewis acidity and the slight suppression of the reducibility at these low K/Mo molar ratios. However, these "secondary" effects are caused by the electronic and structural nature of the active oxygen species of the catalyst [23].

3.2. Differential scanning calorimetry (DCS)

DSC thermograms were obtained over the Si:Ti 1:1 support and molybdena catalysts with K/Mo molar ratios of 0, 0.07, and 0.3. The DSC thermogram for 10% (K/Mo = 0.07)/Si:Ti 1:1 is shown in Fig. 2. The first peak is associated with a combination of the irreversible and reversible adsorption of propylene at 150 °C. After a steady baseline was obtained, the flow was switched to nitrogen only and that propylene which was reversibly adsorbed was allowed to desorb. This switching process was continued until the adsorption and desorption peaks matched, indicating that the surface was saturated with irreversibly adsorbed propylene. The thermogram obtained for 10% Mo/Si:Ti 1:1 was of similar form, whereas those for the Si:Ti 1:1 support and 10% (K/Mo = 0.3)/Si:Ti 1:1 showed only reversible adsorption. Correcting for the heat capacity difference due to the composition differences, as described in the experimental section, and integrating each individual peak allow the calculation of the heat associated with both the reversible and irreversible adsorption of propylene over the samples. Results are shown in Table 2. As can be seen, there was only reversible adsorption associated with the Si:Ti 1:1 support. The Mo-only catalyst exhibited the largest heat value associated with the irreversible adsorption of propylene. With the introduction of potassium, K/Mo = 0.07, this value is reduced by roughly

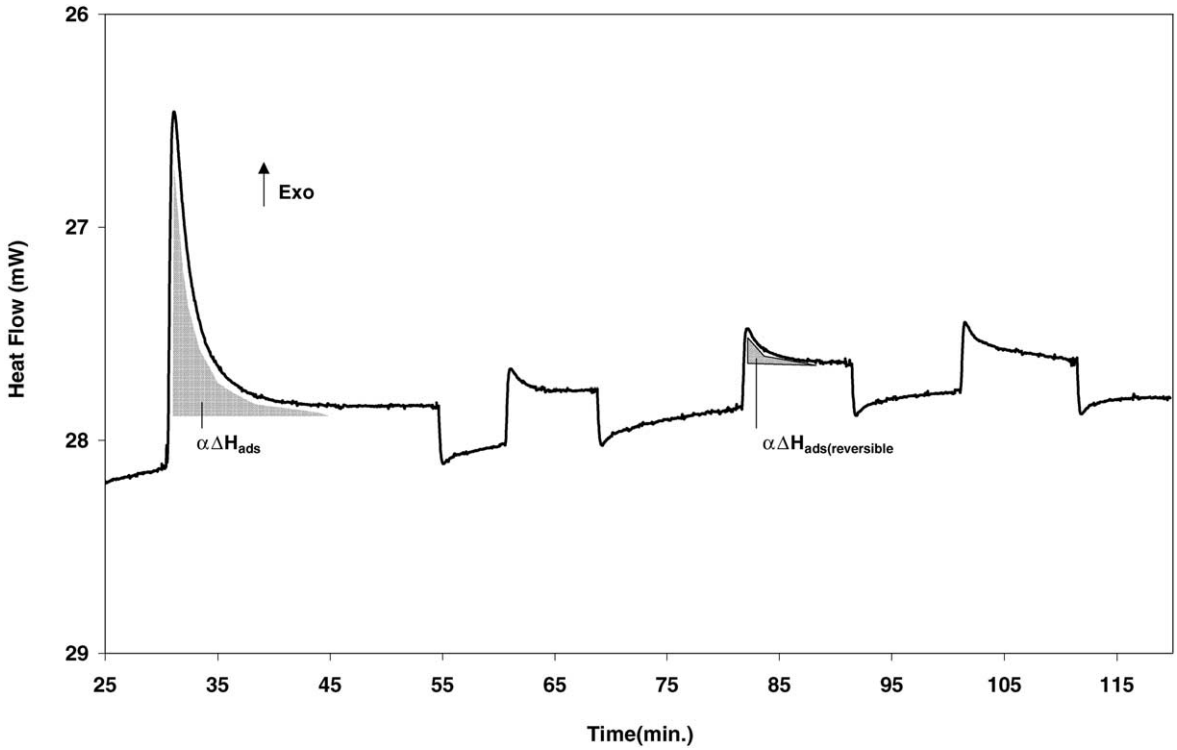

Fig. 2. DSC thermogram obtained for 10% (K/Mo = 0.07)/Si:Ti 1:1 during propylene adsorption/desorption at 150 °C. Flow switch: 5% propylene/nitrogen → nitrogen (25 cc/min).

Table 2
Heat associated with propylene adsorption on Mo/Si:Ti 1:1 catalysts with different K/Mo molar ratios

Sample	Q_{irrev} ($\times 10^4$ mJ/m^2 sample)	Q_{rev} ($\times 10^4$ mJ/m^2 sample)
10% Mo/Si:Ti 1:1	−3.193	−0.126
10% (K/Mo = 0.07)/Si:Ti 1:1	−1.323	−0.065
10% (K/Mo = 0.3)/Si:Ti 1:1	–	−0.036
Si:Ti 1:1	–	−0.020

one third. At K/Mo = 0.3, there was no detectable irreversible adsorption of propane. It can further be noted that the heat associated with the reversible adsorption of propylene is seen to decrease with the addition of potassium. This information further corroborates the relationship between potassium addition and the decreased reactivity for propylene. The addition of alkali promoters leads to electron transfer to the Mo^{6+} cation in MoO_x domains, which become less acidic and show smaller ΔH_{ads} and lower reactivity

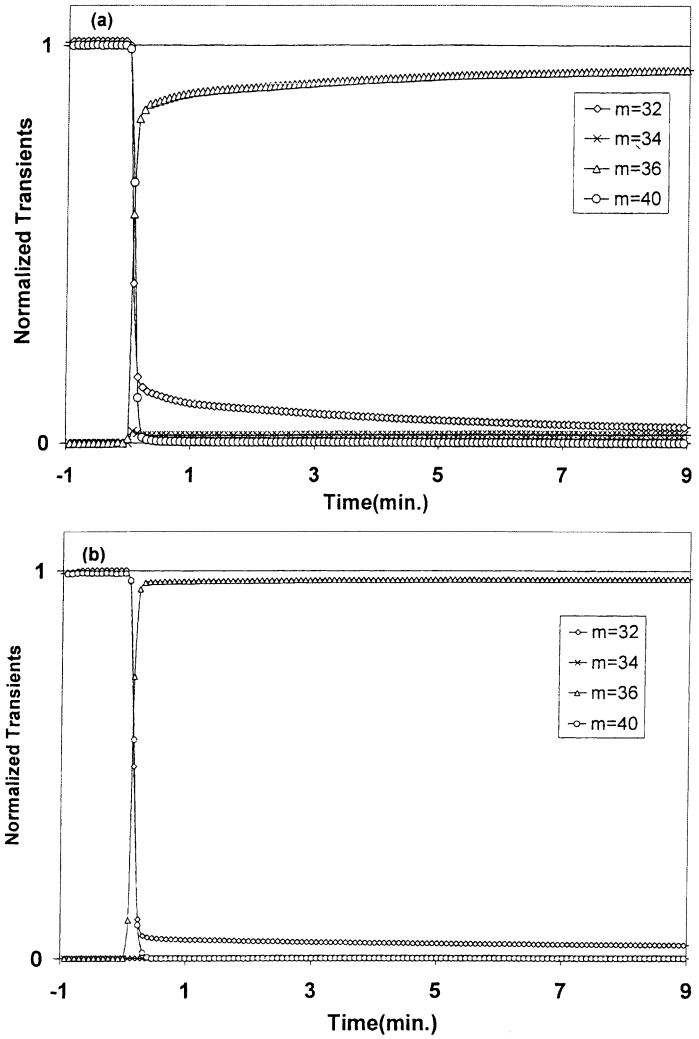

Fig. 3. Oxygen isotopic exchange experiments under steady-state conditions (10% $^{16}O_2$/1% Ar/He → 10% $^{18}O_2$/He) for 10% Mo/Si:Ti 1:1 catalysts with different K/Mo molar ratios: (a) 10% Mo/Si:Ti 1:1; (b) 10% (K/Mo = 0.07)/Si:Ti 1:1; (c) 10% (K/Mo = 0.3)/Si:Ti 1:1.

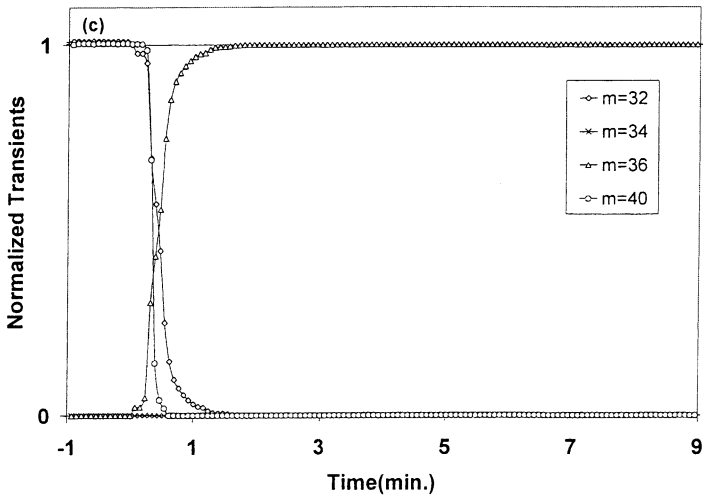

Fig. 3. (*Continued*).

rates for propylene [22]. Even though propane is not as basic as propylene, it is also expected that the addition of alkali will affect the adsorption properties of propane during ODH reactions. To explain the observed increase in propylene formation rates with the introduction of low amounts of alkali in our ODH experiments, it is necessary to also consider the structure of MoO_x domains. Specifically, the interaction of the MoO_x domain with the support can also affect the reactivity of the catalysts and must be taken into account together with the observed effects of alkali on the surface acidity of the catalysts.

3.3. Non-steady-state and steady-state isotopic transient kinetic analysis (SSITKA)

Isotopic oxygen exchange experiments were performed over the Si:Ti 1:1 support and 10% Mo/Si:Ti 1:1 catalysts with K/Mo molar ratios of 0 and 0.3. There was no appreciable exchange detected over the Si:Ti 1:1 support. The transients obtained under steady-state conditions for the remaining samples are shown in Fig. 3. As can be seen, under steady-state conditions, there is only a very small amount of cross-labeled oxygen ($m/z = 34$) observed over the 10% Mo/Si:Ti 1:1 catalyst (Fig. 3a). The transient for cross-labeled oxygen does not relax back to zero during the course of the experiment. The $^{16}O_2$ response transient relaxes quickly, but steadies at a non-zero value, which is always higher than the signal of the cross-labeled oxygen. This behavior suggests that exchange on the surface takes place readily, and the diffusion from the bulk is also contributing to the continued presence of unlabeled oxygen long after the gas stream is switched to $^{18}O_2$. With the addition of potassium (Fig. 3b) the interaction is markedly decreased. There is no cross-labeled oxygen observed and the transient for doubly labeled oxygen relaxes back to zero. However, the oxygen transients relax slower than the argon inert from the beginning of the switch, indicating an interaction with the surface, but possibly a much lower accessibility of oxygen from the bulk of the lattice.

On metal oxides, oxygen may be exchanged by two mechanisms, depending on weather oxygen exchanges one or both of its atoms with the surface of the catalyst. This is thought to be dependent on the density of double vacancies available on the surface as compared to that of the single vacancies [25–27]. The results presented here indicate that both mechanisms are present, to a certain extent, over the supported molybdate catalysts and that these mechanisms are affected by the addition of potassium. With the addition of potassium, the mechanism for the formation of cross-labeled oxygen appears to be suppressed. Potassium addition to the MoO_x catalyst appears to be decreasing lattice

diffusivity as the mechanisms of oxygen exchange are suppressed. Addition of alkali to V_2O_5 catalysts has led to the same conclusion [28]. Additionally, it is possible that the decrease in lattice-oxygen mobility is inter-related to the commonly observed effects on reducibility in alkali-promoted MoO_x catalysts. Martin and Duprex [29] have found a good correlation between oxygen mobility and metal–oxygen bond strength, which in part, can affect reducibility.

Oxygen exchange experiments were performed over the same catalysts under transient conditions. After a pre-calcination step, the samples were evacuated for 1 h at 10^{-7} Torr. The samples were then flushed with helium for 1 h at 500 °C. A flow of 10% $^{18}O_2$ in helium with a small amount of argon (∼1%) was then introduced. Exchange under these conditions showed slightly different results indicating that the oxygen mobility of the catalysts is sensitive to pre-treatment conditions. However, the Si:Ti 1:1 support showed no significant exchange or holdup of oxygen species. The transient responses obtained are plotted in Fig. 4. As Fig. 4a indicates, cross-labeled exchange on 10% Mo/Si:Ti 1:1 is not observed under these conditions. However, the double-exchange mechanism is present and participates throughout the course of the reaction. It is possible that the double vacancies required for the double-exchange are more easily formed during the vacuum treatment, making it possible for this mechanism to dominate. On the catalysts studied, the $^{18}O_2$ signal did not rise as fast as the argon inert, indicating an initial adsorption of oxygen on the surface. Over the potassium-free catalyst, there was also a steady exchange of oxygen as seen in the $^{16}O_2$ transient. When potassium is added to the catalyst, however, there was no oxygen exchange as the signals of both ^{16}O ^{18}O and $^{16}O_2$ were at zero level throughout the experiment (Fig. 4b), although there was an initial uptake of oxygen by the surface over this catalyst as well. Weather the adsorption of oxygen will lead to exchange depends on the nature and availability of the oxygen vacancies. How the mobility of these vacancies can be related to selective or non-selective routes in propane ODH remains to be examined. However, it is found that lattice-oxygen availability and the ability of the catalyst to form cross-labeled oxygen can be significantly influenced by the presence of potassium.

The oxygen exchange experiments give an indication of the influence the presence of potassium has on the mobility of oxygen in the catalysts. However, these results cannot be expected to directly translate to the behavior of the catalysts under reaction conditions. In the presence of propane, under ODH conditions, the catalysts may operate in a slightly reduced state, thereby altering the behavior of the surface. To investigate this behavior, a series of *in situ* oxygen exchange experiments were performed under ODH reaction conditions over the 10% Mo/Si:Ti 1:1 catalysts with K/Mo molar ratios of 0 and 0.3. Our switching experiments show that there was no cross-labeled oxygen forming under ODH conditions (e.g. after the switch 5% propane, 2.5% $^{16}O_2$, 91.5 % He, 1% argon → 5% propane, 2.5% $^{18}O_2$, 92.5 % He). It has been reported that, during propane ODH experiments, the dissociative chemisorption of gas phase oxygen is irreversible, giving rise to no cross-labeled oxygen during propane ODH reactions with $^{18}O_2/^{16}O_2$ mixtures [30]. Our results seem to be in agreement with this observation. However, there was a significant interaction of diatomic oxygen with the catalysts surface, Fig. 5a and b. During the course of the exchange experiment, 10% Mo/Si:Ti 1:1 shows that about 50% of the oxygen exiting the reactor is still $^{16}O_2$ (Fig. 5a). Similar to the exchange experiments without reaction, the addition of potassium suppresses the interaction of gas phase oxygen with the catalyst surface (Fig. 5b). However, the interaction is not totally eliminated, indicating the catalyst must be partially reduced in the presence of propane causing an increase in the exchange as compared to experiments performed with no propane present. Adsorbed oxygen species are often ascribed to unselective transformations of propane during ODH experiments [31]. It is therefore possible that the addition of potassium prevents unselective oxygen species that may form during the re-oxidation of the catalyst surface under ODH conditions. This is indicated by the decrease in lattice-oxygen availability in the presence of potassium in steady-state and in situ experiments. However, it is known that the addition of potassium also decreases the reducibility of the catalyst. This relates to a discussion of a “balance” between opposing effects in which the decreased reducibility of the catalyst may cause the activation of propane to be hindered, but at the same time, unselective transformations are also hindered.

The transients obtained for carbon dioxide species (CO_2^{16}, CO^{16} O^{18}, and CO_2^{18}) are shown in Fig. 6.

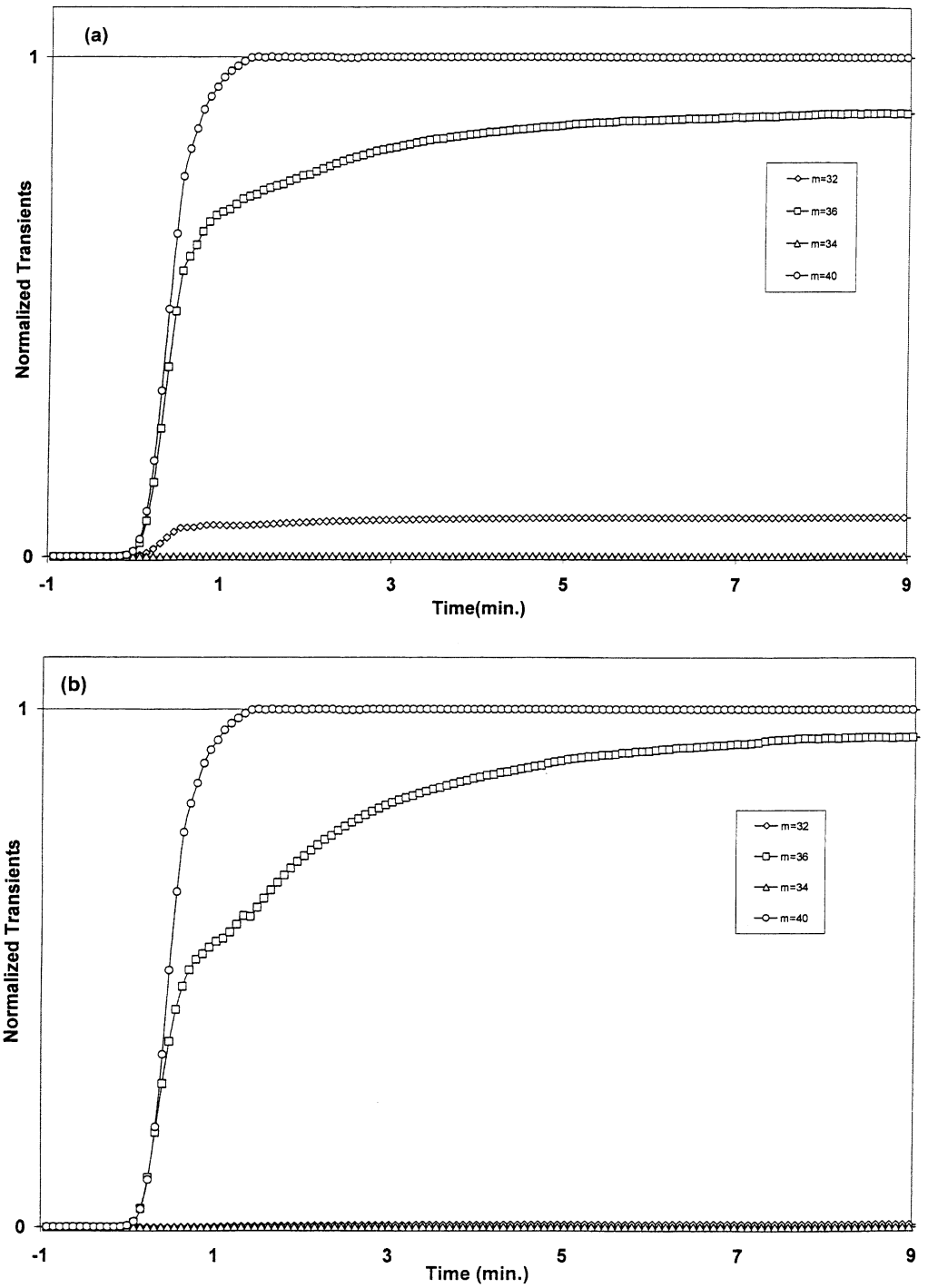

Fig. 4. Oxygen isotopic exchange experiments under transient conditions (He → 10% $^{18}O_2$/He) for 10% Mo/Si:Ti 1:1 catalysts with different K/Mo molar ratios: (a) 10% Mo/Si:Ti 1:1; (b) 10% (K/Mo = 0.3)/Si:Ti 1:1.

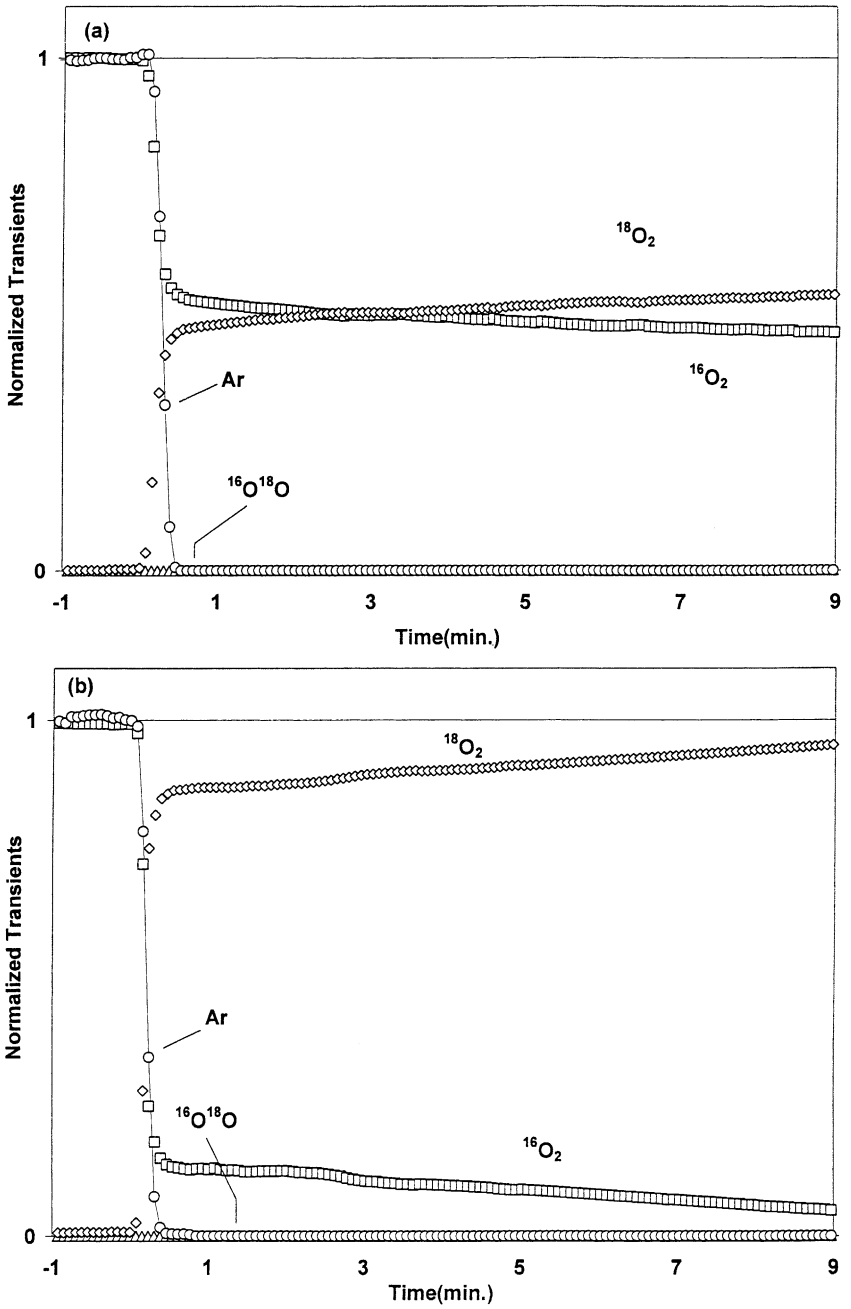

Fig. 5. Oxygen isotopic exchange experiments in the presence of reaction; oxygen transients (2.5% $^{16}O_2$, 91.5% He, 1% argon → 5% propane, 2.5% $^{18}O_2$, 92.5% He) for 10% Mo/Si:Ti 1:1 catalysts with different K/Mo molar ratios: (a) 10% Mo/Si:Ti 1:1; (b) l0% (K/Mo = 0.3)/Si:Ti 1:1.

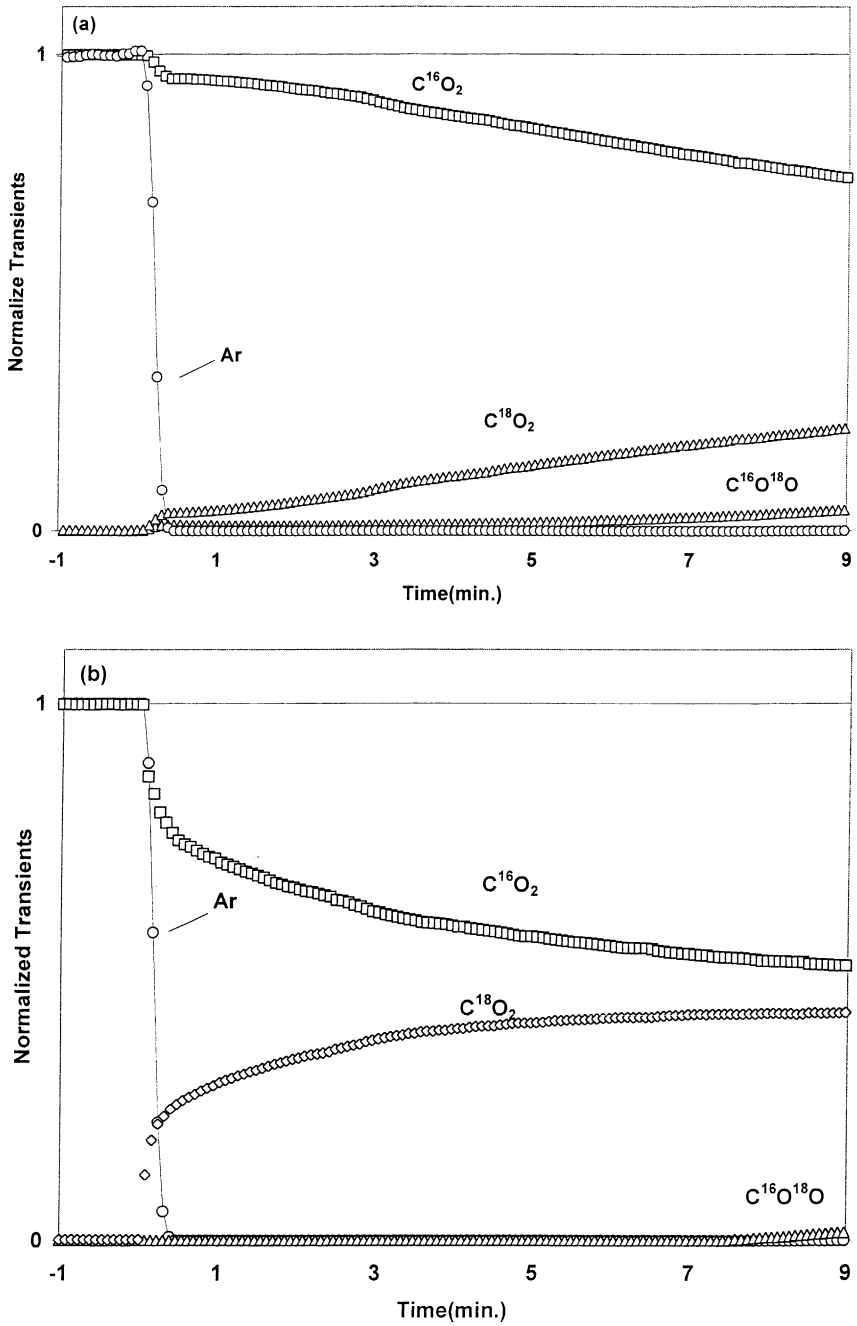

Fig. 6. Oxygen isotopic exchange experiments in the presence of reaction; carbon dioxide transients (2.5% $^{16}O_2$, 91.5% He, 1% argon → 5% propane, 2.5% $^{18}O_2$, 92.5% He) for 10% Mo/Si:Ti 1:1 catalysts with different K/Mo molar ratios: (a) 10% Mo/Si:Ti 1:1; (b) 10% (K/Mo = 0.3)/Si:Ti 1:1.

The steady-state transients obtained for carbon dioxide over 10% Mo/Si:Ti 1:1, Fig. 6a, reveal that O-16 containing carbon dioxide is the pre-dominant isotope for several minutes after the exchange. Both cross-labeled and doubly labeled species rise slowly, the former showing a significant delay before appreciable amounts are formed, ∼5 min. The rate at which the transient for the unlabeled CO_2 species relax is determined by several factors, including the direct incorporation of the lattice-oxygen in a primary combustion reaction to CO_2, the residence time of adsorbed CO_2 species on the surface, the oxygen exchange rate of CO_2 itself with the surface, and the incorporation of oxygen in secondary reaction steps, such as further oxidation of CO to CO_2. The transient for cross-labeled CO_2 could be a due to this secondary reaction. However, another explanation exists in which, as time goes on, the number of ^{16}O atoms on the surface increases and the chance of removing a ^{16}O ^{18}O pair also increases.

The steady-state transients obtained over 10% (K/Mo = 0.3)/Si:Ti 1:1, Fig. 6b, reveal a significant decrease in the participation of the lattice-oxygen in carbon dioxide formation with the addition of potassium to the catalyst, as shown by the faster relaxation of the doubly unlabeled transient. This could also be explained by the much slower replenishment of the unlabeled oxygen on the surface through diffusion from the lattice. There is also a significant lag-time in the formation of cross-labeled carbon dioxide (∼7 min).

It was not possible to precisely account for water transients obtained in the presence of the ODH reaction because molecular water can also participate in lattice exchange. It has been found that water can dissociatively adsorb during ODH reactions [30]. The formation of water in the selective mechanism of propane ODH occurs by the reversible recombination of hydroxyl groups (the most abundant surface species during propane ODH) that are formed from the hydrogen abstraction of propane. These hydroxyls can combine to leave behind vacancies, which are later re-oxidized by gas phase oxygen.

3.4. Electron spin resonance (ESR)

ESR techniques have been widely used to obtain insight into many aspects of the catalysis and surface chemistry of metal oxide surfaces [32]. In particular, calcination of MoO_x catalysts at high temperatures can lead to the formation of paramagnetic Mo(V) centers [33] which can be studied to probe the local environment of the surface-supported species. The adsorption of atmospheric water can have a significant effect on the dispersion and coordination of MoO_x domains and thus, the ESR spectrum. The presence of adsorbed water can cause separation between Mo(V) ions and a consequent sharpening of the ESR line-widths [34]. In this investigation, all samples were maintained in the dehydrated state prior to analysis. Previously dehydrated samples were subsequently purged at 10^{-3} Torr for 30 min after which 100 Torr of propane was introduced. ESR spectra were recorded after 15 min at room temperature under the propane atmosphere. The ESR spectra taken before and after propane adsorption are shown in Fig. 7 for the 10% Mo/Si:Ti 1:1 and the 10% (K/Mo = 0.07) catalyst. A small signal from the superoxide ion (O_2^-) is present in the spectra both before and after contact with propane with a characteristic average g-value of 2.011 [39]. The structural assignment of this species cannot directly be determined, as the superoxide ion can exist and be stabilized both in crystalline TiO_2 [39] and in silica domains [31] as well as being associated with the formation of Mo(V) species. The rather broad spectra are indicative of Mo(V) in a dehydrated oxide matrix [33,34]. The spectra taken before contact with propane (Fig. 7) can be approximated as symmetric (or quasi-axial [35]). Thus, parallel and perpendicular parameter values can be defined as $g_\perp = (g_x + g_y)/2$ and $g_\parallel = g_z$. The g-values for different coordination environments of Mo(V) are reported in literature as follows: 6-coordinate Mo(V), $g_\perp = 1.944$, $g_\parallel = 1.892$; 5-coordinate Mo(V), $g_\perp = 1.957$, $g_\parallel = 1.866$; and 4-coordinate Mo(V), $g_\perp = 1.926$, $g_\parallel = 1.755$ [31,36–38]. The $g_\perp$ and $g_\parallel$ values of Mo(V) in the samples are presented in Table 3. The $g_\perp$ values before propane contact are indicative of hexa-coordinated Mo(V). After contact with propane, the ESR spectra for 10% Mo/Si:Ti 1:1 remains essentially unchanged. However, the spectra for 10% (K/Mo = 0.07)/Si:Ti 1:1 is no longer quasi-axial after adsorption of propane. Keeping in mind that the spectra was taken under a propane atmosphere, it is realized that several species formed from propane could be responsible for the reduction in symmetry of the Mo(V) domains. Since only Mo(V) is detectable in

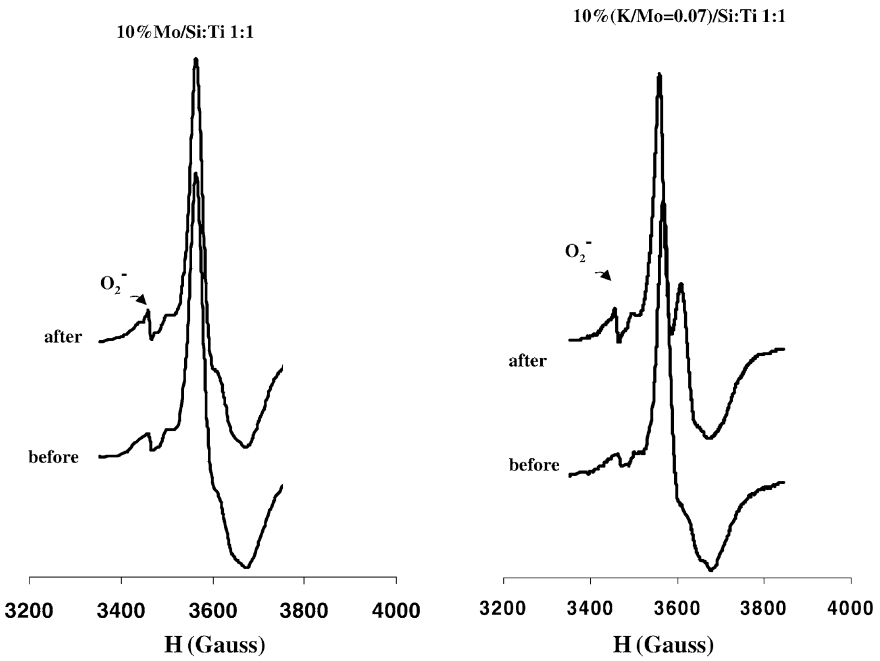

Fig. 7. ESR spectra of 10% Mo/Si:Ti 1:1 and 10% (K/Mo = 0/07)/Si:Ti 1:1 catalysts under dehydrated conditions (before) and after room temperature propane adsorption (100 Torr propane, spectra taken under propane at room temperature).

the ESR technique, we are not able to directly observe transformation between Mo(VI), Mo(V), and Mo(IV). The integral intensity of Mo(V) in these experiments was not observed to change. Therefore, a reduction process was not observed. However, the symmetry change observed in the K/Mo = 0.07 sample is very similar to results reported for a molybdenum sample that was exposed to atmospheric water [23]. It is possible that the formation of –OH groups may have occurred from the adsorption of propane. Furthermore, oxygen-containing adsorbates could be formed from the same process. Whatever the cause of the symmetry change, it is clear that propane interacts more strongly with surface of the potassium-containing catalyst in these experiments. This interaction occurs without a specific reduction of MoO_x species. It is therefore concluded that potassium cannot only affect the transformation of propylene, but also change

Table 3
The *g*-tensor of Mo(V) in (K/Mo)/Si:Ti 1:1 catalysts

	Catalyst	$g_\perp$	$g_\parallel$	
Before adsorption (vacuum)	10% Mo/Si:Ti 1:1	1.943	1.900	
	10% (K/Mo = 0.07)/Si:Ti 1:1	1.946	1.895	
After adsorption*	10% Mo/Si:Ti 1:1	1.942	1.890	
		g_x	g_y	g_z
	10% (K/Mo = 0.07)/Si:Ti 1:1	1.927	1.956	1.891

* Under 500 Torr propane atmosphere.

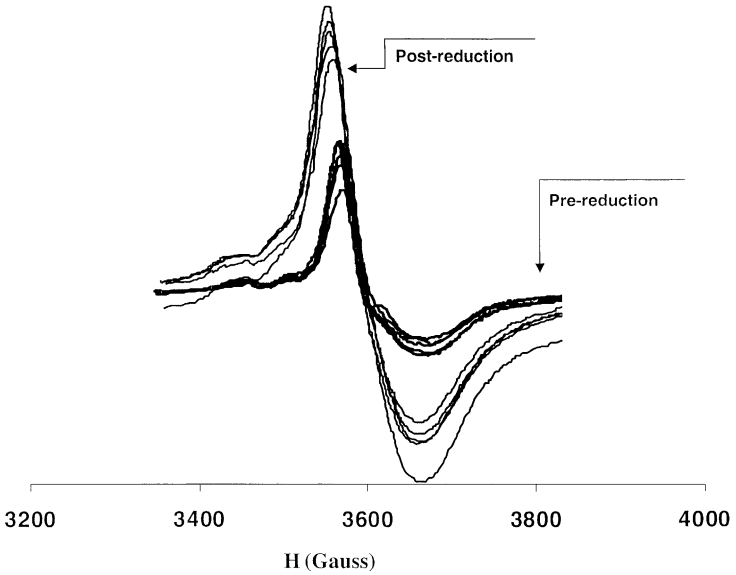

Fig. 8. ESR spectra of 10% Mo/Si:Ti 1:1 catalysts with differing K/Mo molar ratios under dehydrated conditions (before) and after 400 °C propane "reduction" (500 Torr propane, spectra taken after 30 min evacuation at 10^{-3} Torr).

the interaction of the catalyst with propane. This is also consistent with our earlier observation that small quantities of alkali can increase propane conversion, while also improving the propylene selectivity.

To further investigate the effect of potassium on the interaction of propane, a set of propane "reduction" experiments were performed in which the samples were contacted with propane at 400 °C for 30 min and then the system was evacuated for 30 min at 10^{-3} Torr to remove any adsorbed species. The spectra of a series of K/Mo molar ratios (0, 0.035, 0.07, 0.14, and 0.3) are shown in Fig. 8 before and after the reduction. At first glance, it is obvious that an increase in Mo(V) signal intensity has occurred after the reduction, corresponding to Mo(VI) → Mo(V). After the reduction with propane, the spectra remains quasi-axial and the perpendicular and parallel values of the *g*-tensor are given in Table 4. It can be seen that, after the reduction, the *g*-values change and match that of a penta-coordinated Mo(V) species, as described above ($g_\perp = 1.957$), as opposed to the hexa-coordinated Mo(V) species observed before reaction. We cannot, however, resolve whether this shift is due to reduction of Mo(VI) species to penta-coordinated Mo(V) species or to the coordination change of the existing Mo(V) species. It should be recognized that the ESR data obtained for the coordination of Mo(V) centers cannot be directly extrapolated to characterize the coordination environment of the vast majority of Mo(VI) present in the fully oxidized catalysts. While the extent of participation of Mo(V) and Mo(VI) species cannot be determined, it is apparent that Mo(V) contributes to the

Table 4
The *g*-tensor of Mo(V) in (K/Mo)/Si:Ti 1:1 catalysts

Catalyst	$g_\perp$	$g_\parallel$
Dehydrated conditions		
10% Mo/Si:Ti 1:1	1.943	1.900
10% (K/Mo = 0.035)/Si:Ti 1:1	1.945	1.900
10% (K/Mo = 0.07)/Si:Ti 1:1	1.946	1.895
10% (K/Mo = 0.14)/Si:Ti 1.1	1.944	1.907
10% (K/Mo = 0.3)/Si:Ti 1:1	1.940	1.905
After propane (reduction)[a]		
10% Mo/Si:Ti 1:1	1.956	1.868
10% (K/Mo = 0.035)/Si:Ti 1:1	1.955	1.867
10% (K/Mo = 0.07)/Si:Ti 1:1	1.955	1.867
10% (K/Mo = 0.14)/Si:Ti 1:1	1.953	1.866
10% (K/Mo = 0.3)/Si:Ti 1:1	1.953	1.866

[a] 500 Torr propane contact at 400 °C for 30 min followed by vacuum at 10^{-3} Torr for 30 min, spectra taken under vacuum.

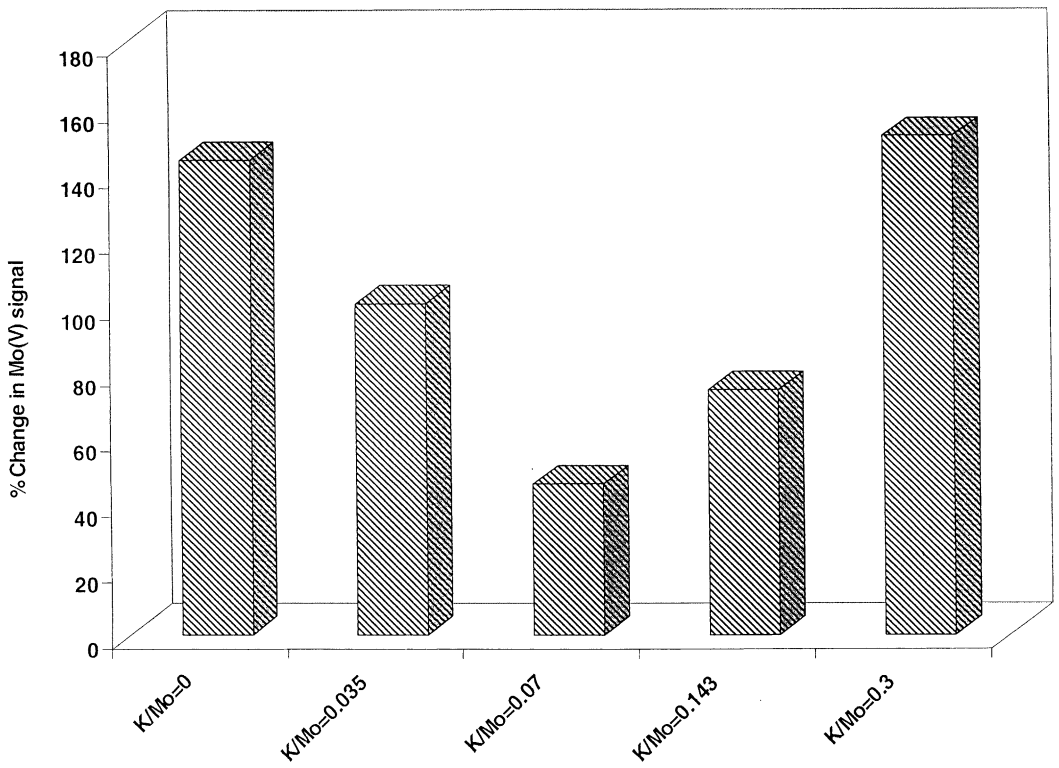

Fig. 9. Percentage change in Mo(V) signal intensity associated with 400 °C propane "reduction" for the 10% Mo/Si:Ti 1:1 catalysts with differing K/Mo molar ratios.

propane transformation and is affected by the addition of potassium. Our earlier studies which showed a positive correlation between the concentration of Mo(V) sites and the propylene yield in propane ODH reaction [23] strongly suggest that Mo(V) species play an important role in the selective transformation of propane.

The integral intensity of the Mo(V) signal is seen to increase to different extents depending on the K/Mo molar ratio. The percentage change in the signal after propane "reduction" is given in Fig. 9, which shows that the K/Mo = 0.07 catalyst experiences the smallest change in Mo(V) signal. MoO_x based catalysts are often believed to operate effectively under reduced conditions where the presence of Mo(V) is essential [11,32]. Furthermore, it has been claimed that Mo(V) is the active site in propane ODH and other oxidation reactions over MoO_x based catalysts [32,40–43]. Although it is apparent that the presence of Mo(V) plays an important role in selective performance of the catalyst, it also appears that there is an "optimum" concentration of these sites, which coincides with a low loading level of potassium.

3.5. Diffuse reflectance Fourier transform infrared spectroscopy (DRIFTS)

DRIFTS spectra were recorded over the catalysts with K/Mo molar ratios of 0 and 0.07. Spectra were taken after propane and propylene adsorption, under a continuous stream of 1% O_2 in helium flow at various temperatures (150, 200, 250, 300, 350 °C) to investigate the differences in carbon–oxygen containing species present on the catalyst surface. The results for these Temperature Programmed Reaction (TPRxn) studies using DRIFTS after propane adsorption are shown in Fig. 10 in the typical carbon–oxygen frequency range (1900–1300 cm^{-1}). The main feature of Fig. 10 is that the catalyst containing potassium shows

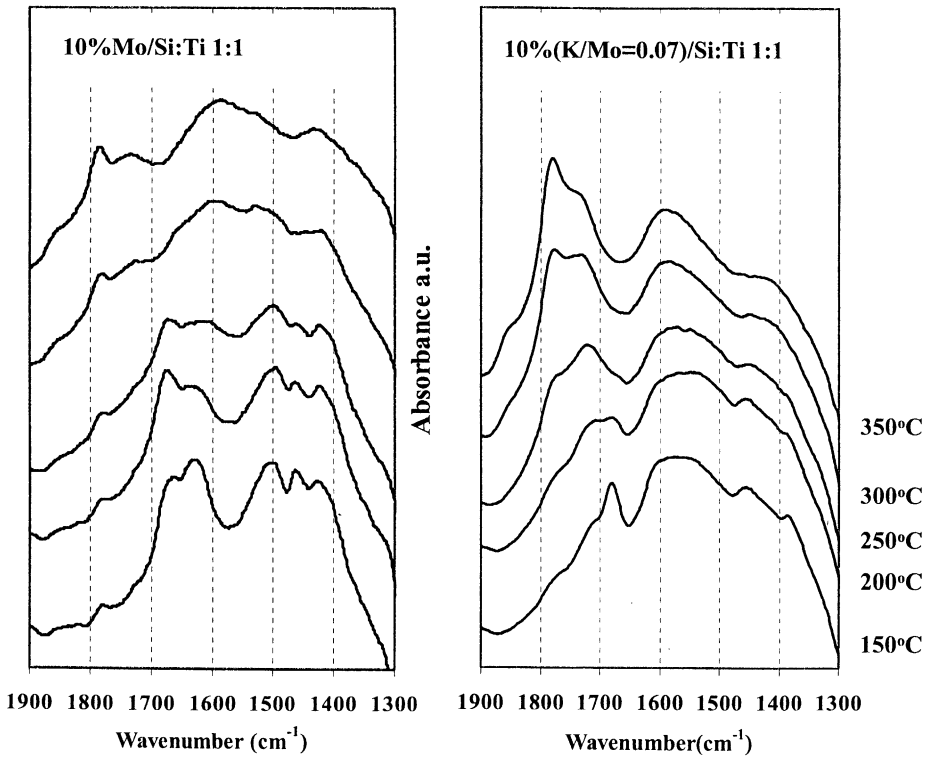

Fig. 10. In situ DRIFT spectra of over 10% Mo/Si:Ti:1:1 catalysts with K/Mo ratios of 0 and 0.07 at different temperatures following propane adsorption. Spectra taken under 1% O_2/He.

large differences in the carbon–oxygen containing species formed after the adsorption of propane when compared to the Mo-only catalyst in the 150 °C spectra. Bands arising from olefinic CH_x stretches are located at 1458 and 1390 cm^{-1} [44,45] and observed on both samples. While this is an indication that propylene has formed on both samples, on the Mo-only catalyst, these bands are convoluted with a feature arising from a bicarbonate species present at 1450 cm^{-1}, which also has a band at 1620 cm^{-1} [47]. Present over both samples is a band located at ∼1675 cm^{-1} associated with adsorbed acetone [47–50]. Conjugated C=O and C=C vibrations are present in the range 1580–1660 cm^{-1} [51] and could arise from a mixture of formate and acetate species. As the temperature is raised, the bands associated with C=O vibrations grow in size as the olefinic CH_x stretches disappear. Bands located at 1780 cm^{-1} are associated with surface carbonate, while bands at 1726 cm^{-1} are assigned to aldehydic C=O vibrations [51–53]. At the highest temperature, 350 °C, the predominate bands arise from carbonates and formate/acetate species. The catalyst containing potassium shows the largest contribution of carbonate species at 350 °C.

The DRIFTS spectra of the K/Mo = 0 and 0.07 samples after propylene adsorption are shown in Fig. 11. One interesting observation emerging from propane and propylene adsorption experiments is that the spectra arising from propane adsorption (Fig. 10) is virtually identical to that arising from propylene adsorption (Fig. 11) over the catalyst containing potassium. This could be an indication that propylene is more readily formed from propane over this catalyst at 150 °C. Over the K-free catalyst, however, the two corresponding spectra are quite different. This is in agreement with the ESR data, which suggested that, at low temperature, propane interacts much more strongly with the alkali containing catalyst. At 150 °C,

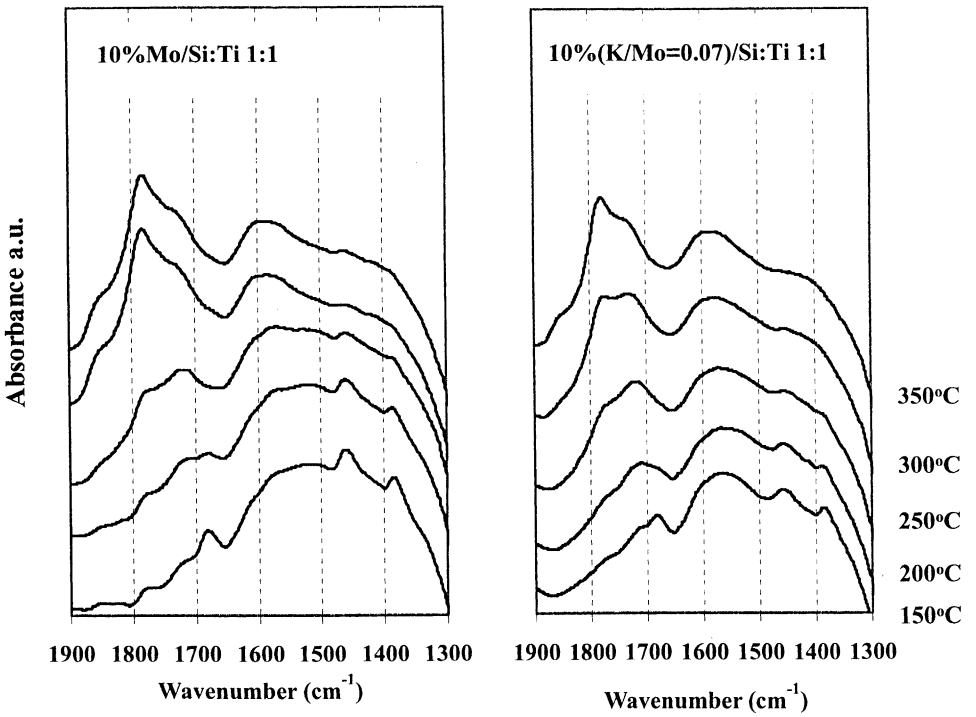

Fig. 11. In situ DRIFT spectra of over 10% Mo/Si:Ti 1:1 catalysts with K/Mo ratios of 0 and 0.07 at different temperatures following propylene adsorption. Spectra taken under 1% O_2/He.

the bands arising from olefinic CH_x are more prominent in both samples around 1458 and 1390 cm^{-1}. However, when compared to the propane adsorption experiments, the bands arising from acetone ($\sim$1675 cm^{-1}) are much weaker. Again, as temperature is raised, the prominent species present on the surface of the two samples is a mixture of carbonates and acetate/formate species.

It is often assumed that the selective activation of propane for propane ODH takes place on the central methylene C–H bond (at the C_2 carbon) and the sequential activation of the product propylene takes place at the allylic C–H bond of this molecule. Intuitively, these are the weakest bonds in each molecule. Unselective transformation of hydrocarbons (combustion) has been extensively studied by Busca and coworkers [45–50]. It was found that acetates and formates are the most likely precursors for CO_x formation. Furthermore, experiments comparing propane and isopropanol adsorption have shown that an isopropoxide species is a likely surface intermediate in the propane ODH reaction [54]. This isopropoxide species was found to readily transform to acetone, which can subsequently further oxidize to formate and acetate species. Although the information obtained in the DRIFTS experiments is of a qualitative nature, one conclusion that can be made is that the activation of propane to form propylene appears to occur more readily over the catalyst containing potassium. The differences in the carbon–oxygen region of the DRIFTS spectra indicate that different, and perhaps unselective, mechanistic steps take place on the Mo-only catalyst and that they are suppressed by the addition of potassium. While most of the effects of alkali promotion have been characterized in terms of the reactivity of the formed propylene, it is conceivable that this alone is not sufficient to explain the difference in the catalytic performance. It is quite likely that the addition of potassium not only affects the reactivity of propylene by making it more stable, it also impacts the propane activation step. The IR data, which do not exhibit a significant difference between the two catalysts following

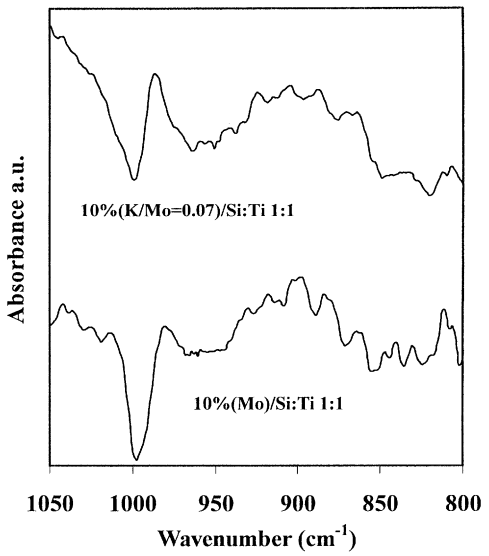

Fig. 12. Difference DRIFT spectra (after propane TP-reaction – before propane TP-reaction) for 10% Mo/Si:Ti 1:1 catalysts with K/Mo ratios of 0 and 0.07 showing participation of molybdenum–oxygen bonds during the experiment.

propylene adsorption, while there was a major difference following propane adsorption, seem to suggest that the effect of potassium on the propane activation step may be just as important as its effect on propylene reactivity, especially under excess oxygen conditions.

When the difference spectrum is obtained by subtracting the spectrum taken before propane adsorption from that taken after propane TPrxn, a direct involvement of the molybdenum oxygen bonds in the sample is recognized (Fig. 12). In the frequency range ~1000–950 cm^{-1}, a negative peak is observed indicating a loss of Mo=O species. Furthermore, in the frequency range typical of Mo–O–Mo vibrations, ~820–850 cm^{-1}, there is also evidence of participation of these molybdenum-oxo bonds during the experiment. Thus, even under an oxygen-containing atmosphere, the participation of molybdenum–oxygen bonds is evident. There appears to be a somewhat larger contribution of Mo=O species over the K/Mo = 0.07 catalyst. This would be consistent with previous data, suggesting that several types of supported species may be created with the addition of alkali that are due to differences in the interaction of MoO_x species with the binary oxide support [23]. The difficulty in ascribing these active oxygen species to a particular catalytic functionality arises from the fact that metal oxide systems commonly posses numerous possible crystalline phases and/or dispersed species and the active and selective catalyst compositions often are reported to contain several of these. Wachs [55] has extensively studied the nature of M–O–M and Mo=O bonds under a variety of conditions. Through ex situ and in situ Raman spectroscopy, it was found that adsorption of water greatly affects the location of the Raman bands (i.e. strength of the bonds) associated with the M=O bonds of vanadium and molybdenum compounds. At high conversions of propane, where significant quantities of water would be formed and re-adsorbed, it is conceivable that the nature of the Mo=O sites may be in a very dynamic state, with multiple processes of adsorption/desorption, oxidation/reduction and lattice-oxygen diffusion occurring simultaneously. Hence, there may be considerable surface re-structuring occurring over the course of reaction. In addition to bridging and terminal oxygen sites of the lattice, upon dissociative adsorption of molecular oxygen, anionic species (O_2^-, O^-) can also form. These can then be inserted into propane in a non-selective manner through electrophillic addition. It has been shown [56,57], that C=C bond breaking prevails when there is an abundance of adsorbed oxygen present at the surface during propane ODH. Furthermore, the partially reduced oxygen species mentioned can be produced at the surface of molybdenum oxides and were found to contribute to total oxidation [58]. The present data indicate that the addition of potassium can significantly alter the interaction between gas-phase and lattice-oxygen, even under propane ODH conditions.

4. Conclusions

Several effects are induced upon low-level alkali doping of molybdate-based catalysts in the adsorption and reactivity of propane and propylene under various conditions. Furthermore, the addition of potassium decreases the amount of available (lattice) oxygen as seen through the use of non-steady-state and steady-state isotopic transient kinetic analysis (SSITKA). It is possible that the addition of potassium inhibits desorbable oxygen species that may be

associated with unselective conversion of propane or propylene. Alkali promotion can account for a "balance" of effects on propane ODH catalysts, in which the decreased reducibility of the catalyst may cause the activation of propane to be suppressed, but at the same time, unselective transformations are also hindered. This is readily observed in DSC experiments, in which the adsorption strength of propylene is decreased with the addition of potassium to the catalysts. These combined effects contribute to the maximum in propylene yield observed with K/Mo molar ratio over the samples studied.

ESR experiments suggest that potassium stabilizes the MoO_x domains in a more "reduced" state and that Mo(V) may be an important participant in the activation of propane. This would agree with our previous results where the observed propylene formation rate appeared to correlate with the relative abundance of the Mo(V) species. While most of the effects of alkali promotion have been characterized in terms of the reactivity of the formed propylene, DRIFTS data indicate that, under excess oxygen conditions, the addition of potassium also affects the activation pathway of propane.

Acknowledgements

Financial support provided by the National Science Foundation (Grant CTS-9412544) is gratefully acknowledged.

References

[1] Council for Chemical Research, US DOE, and ACS, Catalyst Technology Roadmap Report: Build Upon Technology Vision 2020: The US Chemical Industry, ACS Workshop, Washington, DC, USA, 1997.
[2] H.H. Kung, Adv. Catal. 40 (1994) 1.
[3] E.A. Mamedov, V. Cortés-Corberan, Appl. Catal. 127 (1995) 1.
[4] F. Cavani, F. Trifiro, Catal. Today 24 (1995) 307.
[5] M. Baerns, O. Buyevskaya, Catal. Today 45 (1998) 13.
[6] A. Khodakov, J. Yang, S. Su, E. Iglesia, A.T. Bell, J. Catal. 177 (1998) 343.
[7] A. Khodakov, B. Olthof, A.T. Bell, E. Iglesia, J. Catal. 181 (1999) 205.
[8] K. Chen, S. Xie, E. Iglesia, A.T. Bell, J. Catal. 189 (2000) 421.
[9] K. Chen, S. Xie, E. Iglesia, A.T. Bell, J. Catal. 198 (2001) 232.
[10] K. Chen, S. Xie, E. Iglesia, A.T. Bell, J. Phys. Chem. 104 (2000) 1292.
[11] R. Schlogl, A. Knop-Gericke, M. Havecker, U. Wild, D. Frickel, T. Ressler, R.E. Jentoft, J. Wienhold, G. Mestl, A. Blume, O. Timpe, Y. Uchida, Top. Catal. 15 (2001) 219.
[12] A. Pantazidis, A. Auroux, J.-M. Herrmann, C. Mirodatos, Catal. Today 32 (1996) 81.
[13] M.M. Bettahar, G. Costentin, L. Savary, J.C. Lavalley, Appl. Catal. 145 (1996) 1.
[14] W.D. Mross, Catal. Rev.-Sci. Eng. 25 (4) (1983) 591.
[15] C.L. O'Young, J. Phys. Chem. 93 (1989) 2016.
[16] R. Grabowski, B. Grzybowska, K. Samson, J. Sloczynski, J. Stoch, K. Wcislo, Appl. Catal. 125 (1995) 129.
[17] M.F. Portela, R.M. Martin-Aranda, L.M. Madeira, F. Friere, M. Oliveira, Appl. Catal. 127 (1995) 201.
[18] C. Martin, I. Martin, V. Rives, B. Grzybowska, I. Gressel, Spectrochim. Acta Part A 52 (1996) 733.
[19] S.A. Driscoll, D.K. Gardner, U.S. Ozkan, J. Catal. 147 (1994) 379.
[20] M.C. Abello, M.F. Gomez, L.E. Cadus, Catal. Lett. 53 (1998) 53.
[21] A.A. Lemonidou, L. Nalbandian, I.A. Vasalos, Catal. Today 61 (2000) 333.
[22] K. Chen, S. Xie, A.T. Bell, E. Iglesia, J. Catal. 195 (2000) 244.
[23] R.B. Watson, U.S. Ozkan, J. Phys. Chem. 106 (2002) 6930.
[24] R.B. Watson, U.S. Ozkan, J. Catal. 191 (2000) 12.
[25] M.R. Smith, U.S. Ozkan, J. Catal. 142 (1993) 226.
[26] S.A. Driscoll, U.S. Ozkan, J. Phys. Chem. 97 (1993) 11524.
[27] E.R.S. Winter, J. Chem. Soc. Ser. A 23 (1969) 2889.
[28] C. Doornkamp, M. Clement, X. Gao, G. Deo, I.E. Wachs, V. Ponec, J. Catal. 185 (1999) 415.
[29] D. Martin, D. Duprex, J. Phys. Chem. 100 (1996) 9429.
[30] K. Chen, A. Khodakov, J. Yang, A.T. Bell, E. Iglesia, J. Catal. 186 (1999) 325.
[31] D. Creaser, B. Anderson, R.R. Hughes, P.L. Silveston, J. Catal. 182 (1999) 624.
[32] Z. Sojka, M. Che, Surf. Chem. Catal. 3 (2000) 163.
[33] L.E. Cadus, M.C. Abello, M.F. Gomez, J.B. Rivarola, Ind. Eng. Chem. Res. 35 (1996) 14.
[34] A.V. Kucherov, T.N. Kucherova, A.A. Slinkin, Micropor. Mater. 26 (1998) 1.
[35] A.V. Kucherov, A.A. Slinkin, Catal. Lett. 64 (2000) 53.
[36] D. Boudlich, M. Haddad, A. Nadiri, R. Berger, J. Kliava, J. Non-Cryst. Solids 224 (1998) 135.
[37] Z. Sojka, A. Adamski, M. Che, J. Mol. Catal. 112 (1996) 469.
[38] C. Louis, M. Che, M. Anpo, J. Catal. 141 (1993) 453.
[39] M. Che, Z. Sojka, Top. Catal. 15 (2001) 2.
[40] Q. Xhao, X. Bao, Y. Wang, L. Lin, G. Li, X. Guo, X. Wang, J. Mol. Catal. 157 (2000) 265.
[41] M.C. Abello, M.F. Gomez, L.E. Cadus, Catal. Lett. 53 (1998) 185.
[42] B. Zhang, N. Liu, Q. Lin, D. Jin, J. Mol. Catal. 65 (1991) 15.
[43] L.E. Cadus, M.F. Gomez, M.C. Abello, Catal. Lett. 43 (1997) 229.
[44] M. Banares, Catal. Today 51 (1999) 319.

[45] G. Busca, E. Finocchio, V. Lorenzelli, G. Ramis, M. Baldi, Catal. Today 49 (1999) 453.
[46] M. Baldi, F. Milella, G. Ramis, V.S. Escribano, G. Busca, Appl. Catal. 166 (1998) 75.
[47] V. Ermini, E. Finocchio, S. Sechi, G. Busca, S. Rossini, Appl. Catal. 190 (2000) 157.
[48] V. Ermini, E. Finocchio, S. Sechi, G. Busca, S. Rossini, Appl. Catal. 198 (2000) 67.
[49] M. Baldi, V.S. Escribano, J.M.G. Amores, F. Milella, G. Busca, Appl. Catal. 17 (1998) L175.
[50] E. Finocchio, G. Busca, V. Lorenzelli, R.J. Willey, J. Catal. 151 (1995) 204.
[51] V.A. Matyshak, O.V. Krylov, Catal. Today 25 (1995) 1.
[52] M.C. LaNeve, X. Lei, T.P. Fehiner, E.E. Wolf, J. Catal. 177 (1998) 11.
[53] J.E. Sambeth, M.A. Centeno, A. Paul, L.E. Briand, H.J. Thomas, J.A. Odriozola, J. Mol. Catal. 161 (2000) 89.
[54] M. Baldi, E. Finocchio, C. Pistarion, G. Busca, Appl. Catal. 173 (1998) 61.
[55] I.E. Wachs, Catal. Today 27 (1996) 437.
[56] O.V. Buyevskaya, M. Baerns, Catal. Today 42 (1998) 315.
[57] H.W. Zanthoff, S.A. Buchholz, A. Pantazidis, C. Mirodatos, Chem. Eng. Sci. 54 (1999) 4397.
[58] G. Busca, Catal. Today 27 (1996) 457.